Cellular Microbiology (2008) **10**(12), 2589–2604
doi:10.1111/j.1462-5822.2008.01233.x
First published online 9 October 2008

Neutrophils recruited to the site of *Mycobacterium bovis* BCG infection undergo apoptosis and modulate lipid body biogenesis and prostaglandin E_2 production by macrophages

Heloisa D'Avila,[1] Natalia R. Roque,[1] Rafael M. Cardoso,[1] Hugo C. Castro-Faria-Neto,[1] Rossana C. N. Melo[2]†† and Patrícia T. Bozza[1]*†**

[1]*Laboratório de Imunofarmacologia, Instituto Oswaldo Cruz, Fundação Oswaldo Cruz, Rio de Janeiro, RJ, Brazil.*

[2]*Laboratório de Biologia Celular, Departamento de Biologia, Universidade Federal de Juiz de Fora, Juiz de Fora, MG, Brazil.*

Summary

Neutrophil influx to sites of mycobacterial infections is one of the first events of tuberculosis pathogenesis. However, the role of early neutrophil recruitment in mycobacterial infection is not completely understood. We investigated the rate of neutrophil apoptosis and the role of macrophage uptake of apoptotic neutrophils in a pleural tuberculosis model induced by BCG. Recruited neutrophils were shown to phagocyte BCG and a large number of neutrophils undergo apoptosis within 24 h. Notably, the great majority of apoptotic neutrophils were infected by BCG. Increased lipid body (lipid droplets) formation, accompanied by prostaglandin E_2 (PGE_2) and TGF-β1 synthesis, occurred in parallel to macrophage uptake of apoptotic cells. Lipid body and PGE_2 formation was observed after macrophage exposure to apoptotic, but not necrotic or live neutrophils. Blockage of BCG-induced lipid body formation significantly inhibited PGE_2 synthesis. Pre-treatment with the pan-caspase inhibitor zVAD inhibited BCG-induced neutrophil apoptosis and lipid body formation, indicating a role for apoptotic neutrophils in macrophage lipid body biogenesis in infected mice. In conclusion, BCG infection induced activation and apoptosis of infected neutrophils at the inflammatory site. The uptake of apoptotic neutrophils by macrophages leads to TGF-β1 generation and PGE_2-derived lipid body formation, and may have modulator roles in mycobacterial pathogenesis.

Received 11 April, 2008; revised 11 July, 2008; accepted 22 August, 2008. For correspondence. *E-mail pbozza@ioc.fiocruz.br; Tel. (+55) 21 2598 4492; Fax (+55) 21 2590 9490. **E-mail rossana.melo@ufjf.edu.br; Tel. (+55) 32 3229 3206; Fax (+55) 32 3229 3216. ††These senior authors have equally contributed to this work.

© 2008 The Authors
Journal compilation © 2008 Blackwell Publishing Ltd

Introduction

Host resistance to mycobacterial infection depends on recruitment and activation of inflammatory cells to sites of infections. Neutrophils are the first phagocytes to appear in the tuberculous exudate, although the accumulation of monocyte/macrophage lineage is predominant with disease progression (Antony *et al*., 1985; Kasahara *et al*., 1998). The roles of early neutrophil recruitment in the course of mycobacterial infection are not completely understood.

Neutrophils seem to be important for early control of bacterial infections because they are able to phagocyte and release potent mediators, initiating the inflammatory response to tuberculous bacilli. However, it is not clear whether these cells have direct protective functions (Fulton *et al*., 2000). The capacity of neutrophils to induce protective or pathogenic response relates to their numbers and activity at the site of disease. It has been demonstrated that neutrophils are activated by mycobacterial antigens and present mycobactericidal potential through reactive oxygen radical production, oxidative killing of intracellular pathogens and antimicrobial peptides (Jones *et al*., 1990; MacMicking *et al*., 1997; Martineau *et al*., 2007). A protective role for neutrophils have been proposed as neutropenia improves the growth of *Mycobacterium avium* (Appelberg *et al*., 1995), neutrophil depletion leads to decreased ability of whole-blood to restrict mycobacterial growth (Martineau *et al*., 2007) and antibody-induced neutrophil depletion leads to increase *Mycobacterium tuberculosis* in lungs (Pedrosa *et al*., 2000). Conversely, Eruslanov *et al*. (2005) demonstrated that neutrophils present poor ability to restrict mycobacterial growth compared with that of lung macrophages, indicating that the prevalence of neutrophils in tuberculous inflammation contributes to development of pathology. Accordingly, depletion of neutrophils resulted in significantly enhanced survival in a susceptible mouse strain infected by *M. tuberculosis* (Keller *et al*., 2006). Higher influx of neutrophils

has been associated to bronchogenic dissemination of *M. tuberculosis* in the lungs of a susceptible strain of mice (Cardona *et al*., 2000). Furthermore, neutrophils migrate in response to mycobacteria, engulf the bacilli and undergo apoptosis in susceptible mice (Aleman *et al*., 2002). Indeed, it has been recently shown that *M. tuberculosis*-induced neutrophil activation leads to the acceleration of apoptosis in neutrophils through mechanisms dependent on TLR2 and p38 MAP kinase (Aleman *et al*., 2004; 2005).

Accumulating evidence demonstrated that neutrophil apoptosis, followed by recognition and clearance of apoptotic bodies, is associated with a downregulation of inflammation and prevents tissue damage (Fadok *et al*., 1998; Huynh *et al*., 2002). Fadok *et al*. (1998) demonstrated that phagocytosis of apoptotic human neutrophils by macrophages triggers the production of TGF-β1 and prostaglandin E_2 (PGE_2). Uptake of apoptotic cells through mechanisms dependent on TGF-β1 and PGE_2 leads to macrophage deactivation and drives the replication of intracellular pathogen (Freire-de-Lima *et al*., 2000; Ribeiro-Gomes *et al*., 2004). In agreement, increased levels of PGE_2 contribute to downregulate cell mediate immunity, enabling disease progression, a phenomenon that could be reverted by treatment with COX-2 inhibitors (Hsueh *et al*., 1979; Hines *et al*., 1995; Freire-de-Lima *et al*., 2000; Rangel Moreno *et al*., 2002).

The mechanisms involved in enhanced PGE_2 generation by apoptotic cells are not completely understood, and may involve regulated expression of eicosanoid-forming enzymes as well as compartmentalization of signalling components within discrete cellular locations. We have recently described that intracellular lipid domains, called lipid bodies, are involved in PGE_2 synthesis during BCG infection and our observations suggest that lipid bodies and lipid body-derived PGE_2 might have implications to the pathogenesis of mycobacterial infection (D'Avila *et al*., 2006; 2007; 2008). In the present study, we used a murine model of pleural tuberculosis induced by *Mycobacterium bovis* Bacillus Calmette-Guérin to demonstrate that mycobacterial infection induces intense neutrophil recruitment and apoptosis. Moreover, we demonstrated that the uptake of apoptotic neutrophils by macrophages elicits increased synthesis of PGE_2 and TGF-β1 by these cells in parallel to increased formation of lipid bodies, intracellular PGE_2-forming sites during BCG infection. These anti-inflammatory mediators act as macrophage deactivation and may favour the bacteria persistence.

Results

Neutrophils rapidly migrate and ingest BCG at the site of infection

Experimentally induced tuberculosis is characterized by an early neutrophil influx, followed by monocyte, lymphocyte and eosinophil influx (Menezes-de-Lima-Junior *et al*., 1997; Werneck-Barroso *et al*., 2000; Penido *et al*., 2003; Aleman *et al*., 2005; Appelberg, 2007). Accordingly, BCG-induced pleurisy model triggered significant cell recruitment at 6 h, rating maximum at 24 h of infection and persisting for 15 days after infection (not shown). At 6 h, the cell infiltrate was predominately composed of neutrophils that rapidly (from 1 to 6 h) migrated to pleural cavity of infected animals (Fig. 1A). After this time, the number of neutrophils progressively reduced and at 15 days of infection neutrophil numbers were not significantly different from controls (Fig. 1A). The percentage of infected neutrophils within 24 h after BCG infection was quantified by flow cytometry (FACS). To that end, animals were infected with PKH-labelled BCG, and neutrophils were gated based on their forward and side scatter. As shown in Fig. 1B, over 60% of the recruited neutrophils were infected with PKH-labelled BCG within 24 h. Indeed, neutrophils recruited to the inflammatory foci were able to rapidly ingest BCG. In Fig. 1C, a representative image of BCG-containing neutrophils observed after Kinyoun's staining at 1 h of infection is shown. In agreement with the findings obtained by flow cytometry, 62% of pleural recovered neutrophils were infected as assessed by the analysis of Kinyoun's stained slides within 24 h of infection. From the infected neutrophils, 42% exhibited one and 58% exhibited two or more bacteria in their cytoplasm (Fig. 1D).

BCG infection induces neutrophil apoptosis

Neutrophils are short-living cells in inflammatory sites, where usually undergo apoptosis and are rapidly removed by macrophages (Haslett, 1997; 1999). The *in vivo* rate of neutrophil apoptosis was investigated. BCG infection was able to induce significant neutrophil apoptosis *in vivo*. Within 24 h of infection, a significant number of the cells that traffic to pleural cavity underwent apoptosis (29.74% of total leukocytes) as observed in Fig. 2A. Inflammatory neutrophils account for a large amount of apoptotic cells (Fig. 2A). As shown in Fig. 2B, 37% of the neutrophils recovered from the pleural cavity within 24 h of infection with PKH-labelled BCG infected animals were Annexin-V FITC-positive indicative of apoptosis. From these Annexin-V FITC-positive neutrophils, 92% were also positive for PKH-labelled BCG, thus confirming that infected neutrophils are the ones that preferentially undergo apoptosis. In contrast, from the population of live neutrophils less than 45% were infected at this time of analysis (Fig. 2B). Apoptotic neutrophils from BCG-infected mice within 24 h of infection exhibited typical apoptotic morphology, such as nuclear condensation, reduced volume and cytoplasm with vacuoles as observed by bright-field microscopy of May-Grünwald-Giemsa-stained slides (Fig. 2C) and are phagocyted by macrophages (Fig. 2D).

© 2008 The Authors

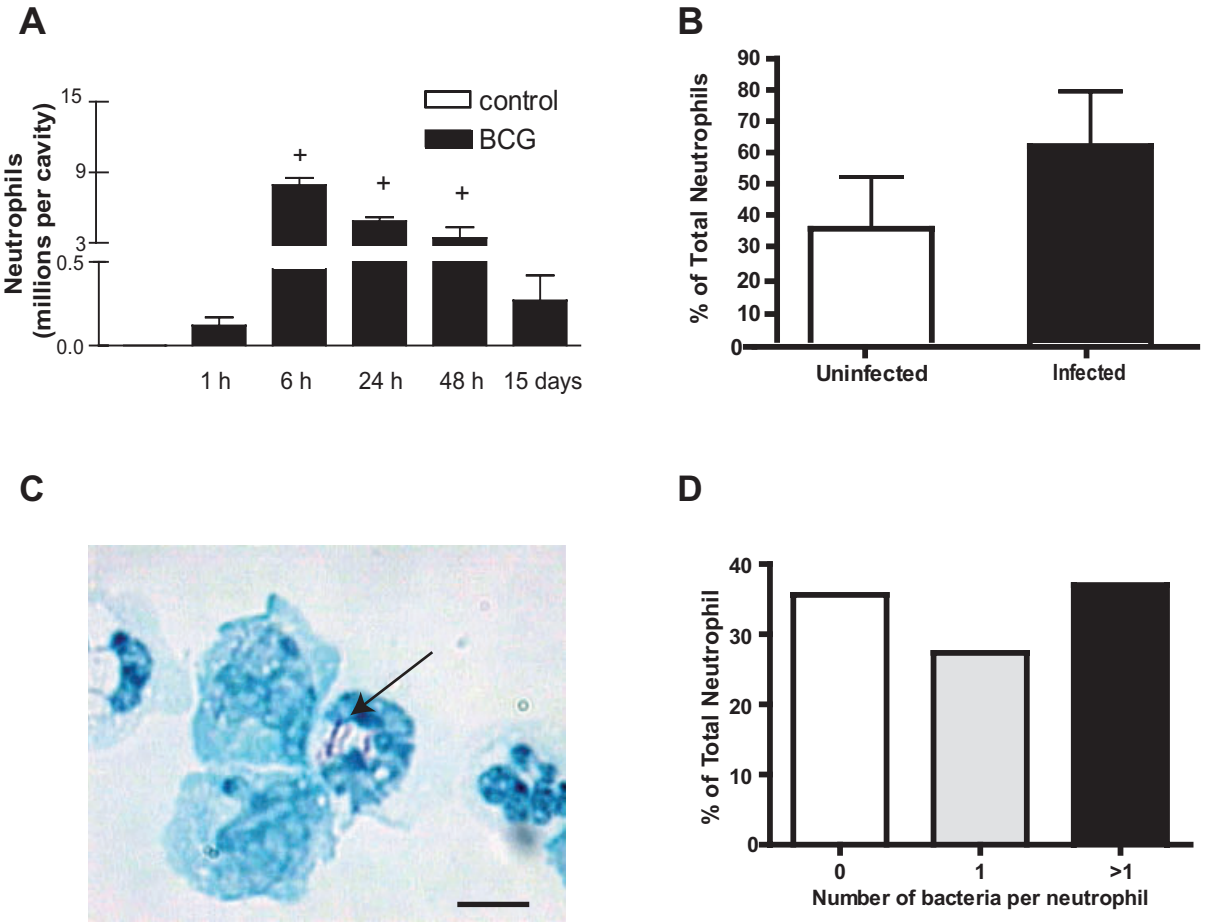

Fig. 1. BCG infection induces time-dependent neutrophil migration in pleural cavities.
A. Kinetic of BCG-induced neutrophil recruitment into pleural cavity.
B. Percentage of uninfected and infected neutrophils at 24 h of infection after FACS analysis of PKH26-stained endocyted BCG.
C. Neutrophils at 1 h of infection exhibiting phagocyted bacteria (arrow) after Kinyoun's staining.
D. Numbers of phagocyted bacteria per neutrophil evaluated within 24 h of infection after Kinyoun's staining.
Bar, 10 μm. C57BL/6 mice were i.pl. infected with BCG (5×10^6 bacilli per cavity). Each bar represents the mean ± SEM from at least five animals. Statistically significant ($P < 0.05$) differences between control and infected groups are indicated by asterisks.

Ultrastructural analysis of infection-induced changes within neutrophils

To characterize ultrastructural alterations within neutrophils in response to BCG infection, pleural cells from infected and non-infected animals were recovered, immediately fixed in a mixture of paraformadehyde and glutaraldehyde, embedded in agar and prepared for transmission electron microscopy (TEM). We have used a technique that enables high contrast of membranes and glycogen particles with optimal visualization of these structures (Dvorak and Monahan-Earley, 1992). Phagocyted bacteria were observed within recruited neutrophils at 1 h of infection (Fig. 3Ai). This means that neutrophils are able to ingest BCG as early as they reach the infection site. Ingested BCG were seen within phagosomes and showed typical morphology (Armstrong and Hart, 1971; Klegerman *et al*., 1996) including a central nuclear region surrounded by an electron-dense cytoplasm. The BCG was surrounded by a typical plasma membrane and a cell wall and an irregular electron-lucent zone that separate each organism from the phagosome-delimiting membrane; the presence of the electron-lucent halo surrounding the bacteria was clearly and very frequently observed within both neutrophils and macrophage-phagocyted neutrophils from the infected group as noted in Fig. 3 (also shown in higher magnification in the boxed area) with a peripheral electron-lucent area (Fig. 3Aii). Free bacteria were not observed within neutrophils. Interestingly, these cells although in suspension were also seen in close association with other cells, suggesting intercellular interaction at the inflammatory site. Figure 3Ai shows a representative image of this phenomenon, also observed in other analyses from the same material. Even being

© 2008 The Authors
Journal compilation © 2008 Blackwell Publishing Ltd,

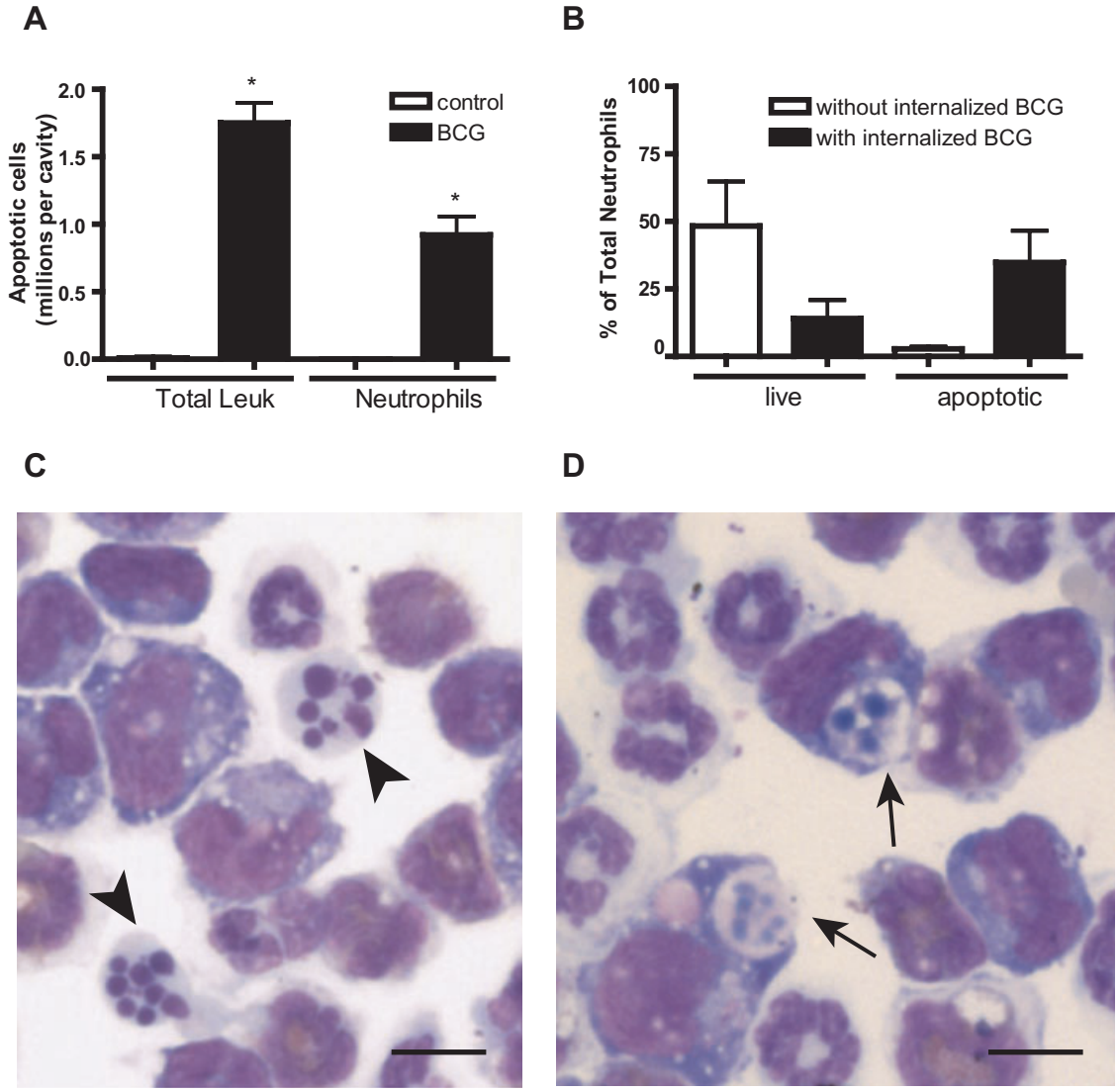

Fig. 2. BCG infection induces apoptosis of pleural cells.
A. Number of total apoptotic leukocytes and apoptotic neutrophils per cavity from control and BCG-infected animals at 24 h.
B. The percentage of live and apoptotic neutrophils containing internalized bacteria or without internalized BCG was assessed in the pleural fluid of BCG-infected animals within 24 h. Apoptosis and infection index were performed by FACS analysis after Annexin-V FITC staining in cells from PKH26-stained BCG-infected group at 24 h.
Each bar represents the mean ± SEM from at least five animals. Statistically significant ($P < 0.05$) difference between control and infected group is indicated by asterisks.
C and D. Bright-field microscopy images exhibiting apoptotic neutrophils (C, arrowheads) and macrophages containing endocyted apoptotic neutrophils (D, arrows) from infected animals at 24 h of infection after May-Grünwald-Giemsa staining. Bar, 10 μm.

in suspension, it was possible to observe attachments between cells; and these attachments (Fig. 3Ai, circles) are considered morphological signals of cell interactions as previously observed between inflammatory cells (macrophages with other immune cells) in infected tissues (Melo and Machado, 1998). The interaction reported in the present work may represent adhesion of neutrophils on the macrophage surface as the initial step for phagocytosis of these cells (Fig. 3Ai, circles). Phagocyted bacteria within neutrophils were also visualized by fluorescence microscopy at 1 h of infection (Fig. 3Bii, arrows), neutrophil infection was quantified and we observed that 61% of neutrophils contained internalized bacteria assessed by fluorescent microscopy with a mean bacteria per neutrophil within 1 h of infection of 1.89 ± 0.59 when 100 cells were analysed from three different infected animals. Remarkably, when these cells were processed for lipid body staining, a large number of fluorescent lipid

© 2008 The Authors

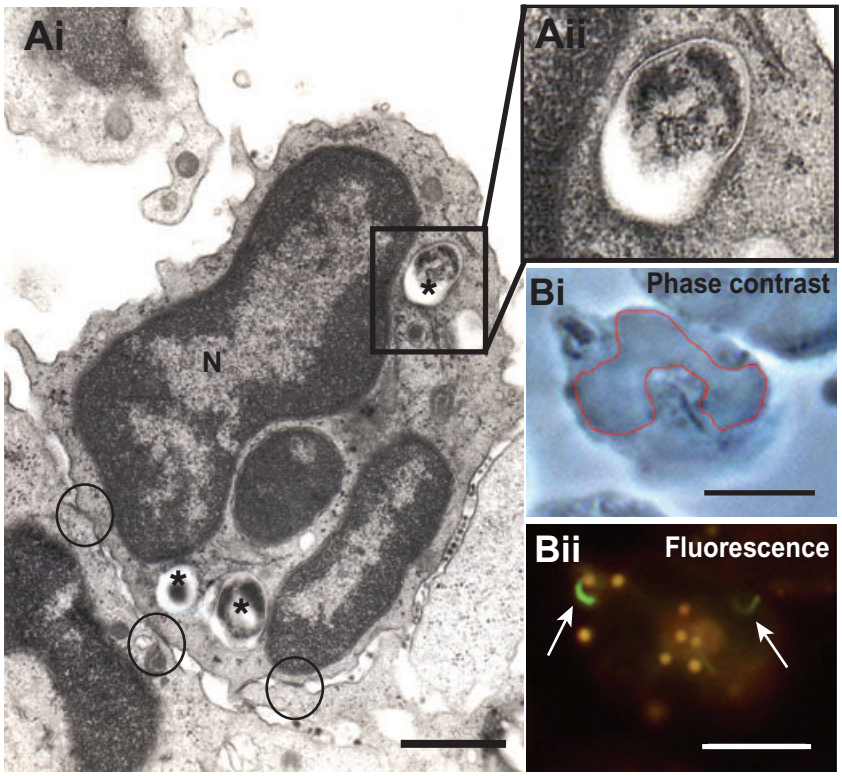

Fig. 3. Inflammatory neutrophils actively ingest bacteria at the sites of infection.
A. (Ai) An infected neutrophil shows phagosomes containing BCG (*) in the cytoplasm, at 1 h of infection. (Aii) corresponds the boxed area of (Ai) and shows an ingested bacterium in high magnification. Areas of interaction between the neutrophil and adjacent cells are indicated (circles).
B. (Bi) Phase-contrast and (Bii) fluorescence microscopy of identical fields of a representative neutrophil at 1 h of *in vivo* infection. Fluorescent Nile Red-labelled lipid bodies were visualized as cytoplasmic yellow punctate inclusions, while phagocyted fluorescent-labelled BCG is imaged in green (arrows). In (Bi), the cell nucleus was outlined. For transmission electron microscopy, pleural cells were fixed in a mixture of glutaraldehyde and paraformadehyde and embedded in agar. Lipid bodies and bacteria were visualized by, respectively, Nile Red or Live/Dead BacLight bacterial viability kit as described in *Experimental procedures*.
Bars, 1 μm (A); 10 μm (B).

bodies, an indicative of cell activation (Bozza *et al.*, 2007), were also detected (Fig. 3Bii) and quantified as significantly enhanced when compared with control non-infected animals (from 1.02 ± 0.02 lipid bodies per neutrophil in control to 6.86 ± 0.65 lipid bodies per neutrophil in BCG-infected animals within 1 h; $n = 3$, $P = 0.05$). In fact, neutrophils at 1 h of infection exhibited ultrastructural features of activation such as higher amount of organelles in conjunction with phagocyted bacteria in the cytoplasm (Fig. 3A, asterisk). However, at 24 h of infection most neutrophils showed degenerative alterations typical of apoptosis. The cells exhibited mild to intense changes imaged mainly as mitochondrial damage and progressive cytoplasmic and nuclear condensation (Fig. 4B and C, arrowhead).

Uptake of infected-apoptotic neutrophils by macrophages stimulates lipid body formation, PGE_2 and TGF-β1 production in vivo

At 24 h of infection, a large number of infiltrating macrophages were observed at the site of infection. These cells showed morphological signals of activation and were actively involved in the phagocytosis of apoptotic neutrophils. Ultrastructural analyses revealed apoptotic neutrophils in different degrees of degeneration inside macrophage phagosomes (Fig. 4A–C, arrowheads). Moreover, macrophages showed a large number of cytoplasmic phagolysosomes containing amorphous or granular materials (Fig. 4B and C, arrows). It is interesting that ingested neutrophils were clearly infected with BCG (Fig. 4B, white arrowhead). Prior observations have demonstrated that phagocytosis of apoptotic cells could affect the PGE_2 synthesis induced by parasite infection (Freire-de-Lima *et al.*, 2000). Recently, we have demonstrated that lipid bodies are the main intracellular sites for PGE_2 synthesis during intracellular pathogen infection (D'Avila *et al.*, 2006). Because they are stores of the eicosanoid precursor (arachidonic acid) in different leukocyte subsets including neutrophils and monocytes (Weller and Dvorak, 1985; Weller *et al.*, 1989; Yu *et al.*, 1998), and contain eicosanoid-forming enzymes (Dvorak *et al.*, 1983; 1992; Bozza *et al.*, 1997; Yu *et al.*, 1998; Pacheco *et al.*, 2002; D'Avila *et al.*, 2006; Accioly *et al.*, 2008), we first investigated the occurrence of lipid bodies within the BCG-elicited macrophages. Figure 5 shows that these cells contain increased numbers of lipid bodies at 24 h when compared with non-infected control animals (Fig. 5A and Di). An ingested bacterium is shown in Fig. 5Di (asterisk), and Fig. 5Dii shows in high magnification a typical apoptotic body. By electron microscopy, macrophages from infected group showed large, electron-lucent, non-membrane bound lipid bodies with a peripheral rim of electron-dense material

© 2008 The Authors

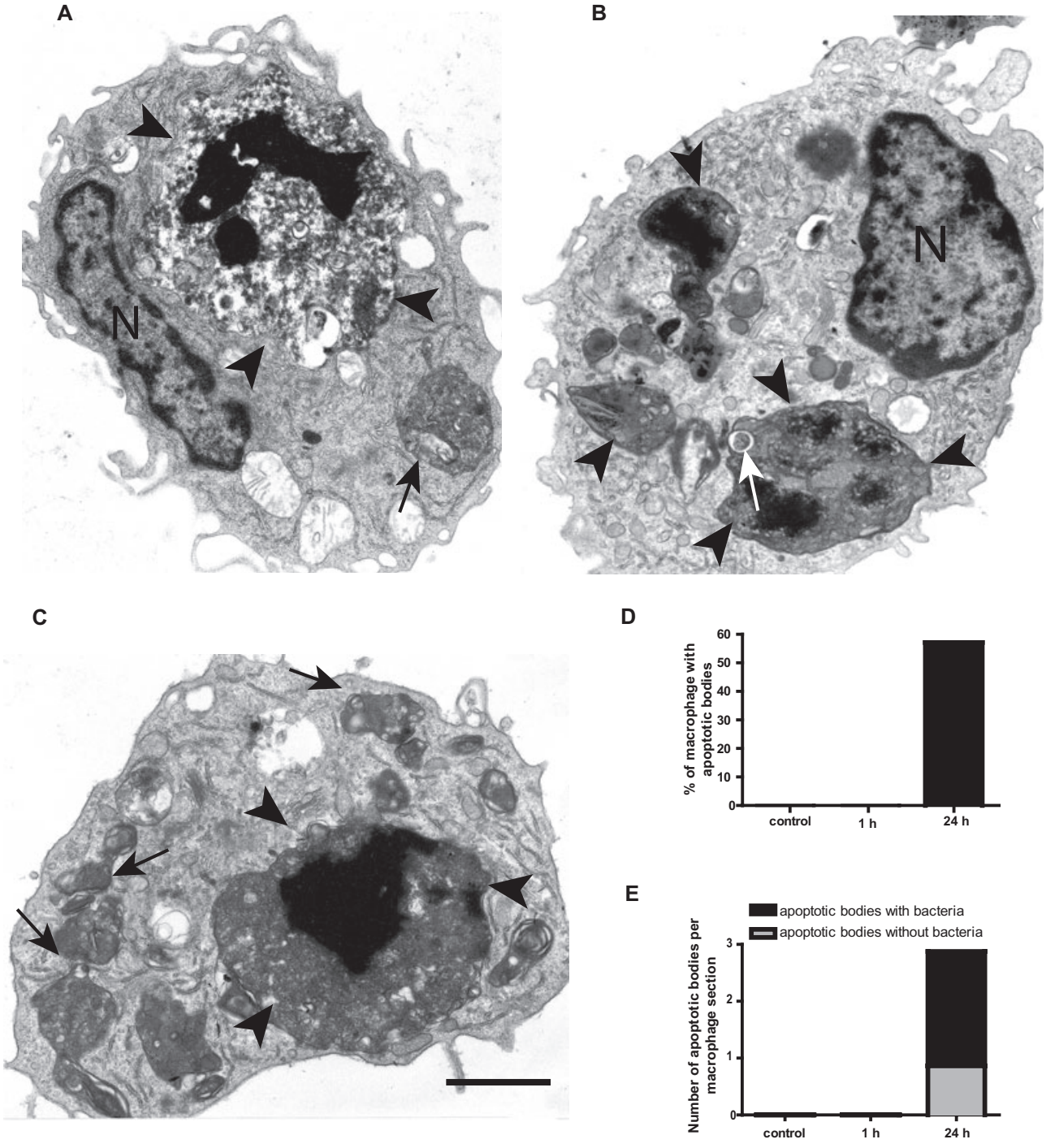

Fig. 4. Phagocytosis of apoptotic neutrophils by inflammatory macrophages.
A–C. Ultrastructural images of inflammatory macrophages at 24 h of infection. Apoptotic neutrophils (arrowheads) are seen in the macrophage cytoplasm in conjunction with a large number of phagolysosomes containing amorphous material (black arrows). In (B), a bacterium (white arrowhead) is clearly observed within a phagocyted neutrophil. N, nucleus. Bar, 1 μm.
D and E. (D) Percentage of macrophages exhibiting apoptotic neutrophils in phagosomes and (E) number of uninfected or infected apoptotic neutrophils per macrophage were enumerated in control and infected groups at 1 and 24 h by TEM. Phagocyted apoptotic cells were counted in 81 macrophage sections showing the entire cell profile and nucleus.

© 2008 The Authors
Journal compilation © 2008 Blackwell Publishing Ltd,

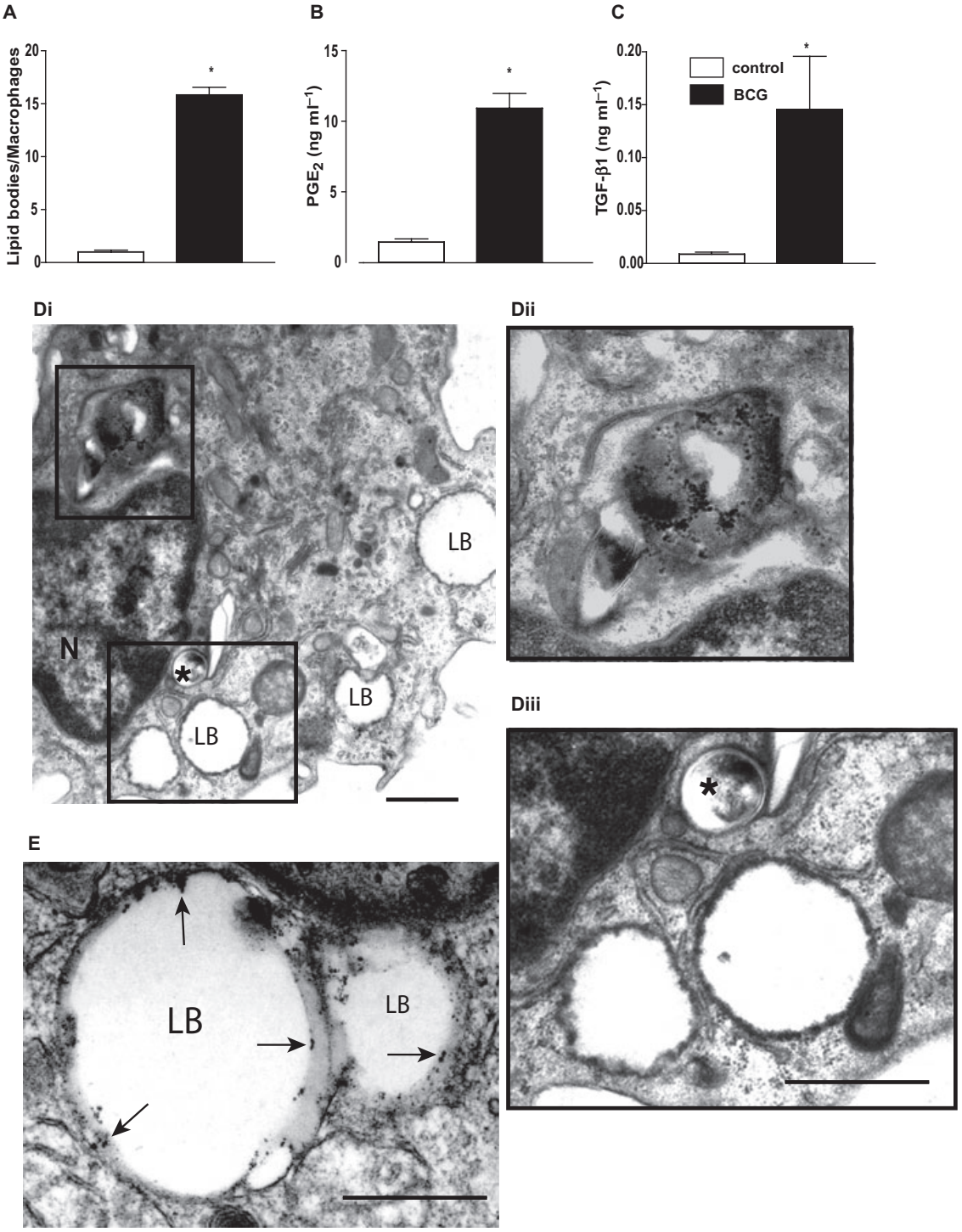

Fig. 5. *In vivo* lipid body formation, PGE_2 and TGF-β1 synthesis occur in parallel to macrophage uptake of apoptotic neutrophils.
A–C. The numbers of lipid bodies within inflammatory macrophages (A) and the levels of PGE_2 (B) and TGF-β1 (C) in the pleural fluid significantly increased compared with non-infected controls at 24 h of infection. Each bar represents the mean ± SEM from at least eight animals. Statistically significant ($P < 0.05$) differences between control and infected groups are indicated by asterisks.
D. (Di) Ultrastructural image of inflammatory macrophage at 24 h of infection. (Dii) and (Diii) correspond the boxed area of (Di) in high magnification. (Dii) shows an ingested apoptotic body and (Diii) revealed cytoplasmic lipid bodies (LB) as electron-lucent, non-membrane-bound organelles with a peripheral electron-dense rim; in (Diii) an ingested bacterium (asterisk) are also observed in the macrophage cytoplasm.
E. Electron-lucent lipid bodies showing positive immunonanogold labelling for ADRP (arrows) in macrophage from infected mice at 24 h.
N, nucleus. Bar, 1 μm.

© 2008 The Authors
Journal compilation © 2008 Blackwell Publishing Ltd,

(Fig. 5Diii). The macrophage lipid bodies shown in Fig. 5 are typical lipid bodies as previously described within macrophages in response to the infection with BCG (D'Avila *et al*., 2006) or *Trypanosoma cruzi* (Melo *et al*., 2003; 2006). We have demonstrated that lipid bodies within pathogen-activated macrophages from different origins (pleura, peritoneum, heart, uterus) change their osmiophilia and can appear as electron-lucent organelles with a peripheral electron-dense rim (Melo *et al*., 2003; 2006; D'Avila *et al*., 2006), as noted in the present work. Newly formed, electron-lucent lipid bodies are predominantly observed in macrophages after 24 h of BCG infection (D'Avila *et al*., 2006). In Fig. 5E, the presence of lipid bodies within infected cells was confirmed by immuno-electron microscopy (EM) using a known marker for lipid bodies – ADRP (adipose differentiation-related protein), a structural protein which is found as a circumferential rim delimiting lipid bodies (reviewed in Bozza *et al*., 2007).

Next, we observed that increased levels of PGE_2 were observed concomitant to lipid body formation within 24 h of infection (Fig. 5B).

Ingestion of apoptotic cells by macrophages also promotes the synthesis and release of cytokines with anti-inflammatory properties (Freire-de-Lima *et al*., 2000). In this context, we also addressed the production of TGF-β1, an important deactivator of the immune response in tuberculosis and parasite infections (Hirsch *et al*., 1997). As observed in Fig. 5C, TGF-β1 was highly produced at 24 h of BCG infection.

Apoptotic neutrophil uptake by macrophages leads to lipid body-derived PGE_2 synthesis

To further characterize if the uptake of apoptotic neutrophils was involved in enhanced lipid body formation and PGE_2 production during BCG infection, murine peritoneal macrophages were co-cultured *in vitro* with living, necrotic or apoptotic neutrophils. At 24 h, we observed that BCG infection and phagocytosis of apoptotic neutrophils significantly increased the number of lipid bodies in macrophages. However no differences were observed between the macrophage co-culture with living or necrotic neutrophil and control groups (Fig. 6A). Moreover, we observed that the uptake of apoptotic neutrophils synergizes with the effects of BCG infection on lipid body formation (mean ± SEM; from 5.9 ± 1.2 lipid bodies per cell in BCG group to 10.16 ± 1.67 BCG plus apoptotic neutrophil group) (Fig. 6A).

We next addressed whether increased numbers of lipid bodies from macrophages stimulated with apoptotic neutrophils would lead to enhanced PGE_2 production. Co-culture of macrophages with apoptotic neutrophils increased the effects of BCG infection on PGE_2 synthesis (mean ± SEM; from 3.6 ± 0.03 ng ml^{-1} in BCG group to 14.0 ± 0.3 ng ml^{-1} in BCG plus apoptotic cell group; Fig. 6B). No differences in PGE_2 levels in the supernatant from control and macrophages co-cultured with living and necrotic neutrophils were observed (Fig. 6B). Unstimulated cells respond by generating low levels of PGE_2; however, the PGE_2 synthetic capacity of macrophages was enhanced after apoptotic neutrophil uptake and paralleled the increased biogenesis of lipid bodies.

NSAIDs, including aspirin and NS398, have been previously shown to inhibit lipid body formation induced through COX-independent mechanisms (Bozza *et al*., 1996; 2002). The capacity of aspirin and NS-398 to inhibit apoptotic cell uptake-induced lipid body formation and PGE_2 synthesis during BCG infection was investigated. As shown in Fig. 6C, both aspirin (5 μM) and NS-398 (1 μM) drastically inhibited BCG-induced lipid body formation within 24 h. As expected, at the concentrations of NSAIDs used, the BCG-induced PGE_2 generation was completely abrogated (Fig. 6D). Recently, we have established a role for lipid bodies in PGE_2 synthesis during BCG infection (D'Avila *et al*., 2006; 2008). In order to gain further insights if the uptake of apoptotic neutrophil-induced lipid bodies has roles in enhanced PGE_2 production, we analysed the effect of a non-cyclooxygenase inhibitor of lipid body biogenesis. To that end, macrophages were treated with fatty acid synthase inhibitor (C75). Treatment with C75 significantly inhibited lipid body formation in macrophages induced by apoptotic cells with or without infection confirming the role of new lipid synthesis in lipid body biogenesis (Fig. 6B). Impairment of lipid body biogenesis by C75 significantly inhibited PGE_2 synthesis induced by apoptotic cells in infected and non-infected macrophages (Fig. 6D).

Inhibition of neutrophil apoptosis partially reduces lipid body formation

To confirm the involvement of apoptotic cells in modulating the BCG infection, mice were intrapleurally (i.pl.) treated with the pan-caspase inhibitor zVAD-fmk peptide immediately before BCG infection. zVAD pre-treatment was not able to affect the neutrophil migration to pleural cavity during infection (Fig. 7C), but rescued neutrophils from death during BCG infection (Fig. 7A). Also, the inhibition of neutrophil apoptosis significantly, although partially, reduced the lipid body formation induced during BCG infection *in vivo* (Fig. 7B). These data corroborate the involvement of apoptotic neutrophil uptake on lipid body formation *in vivo*.

© 2008 The Authors

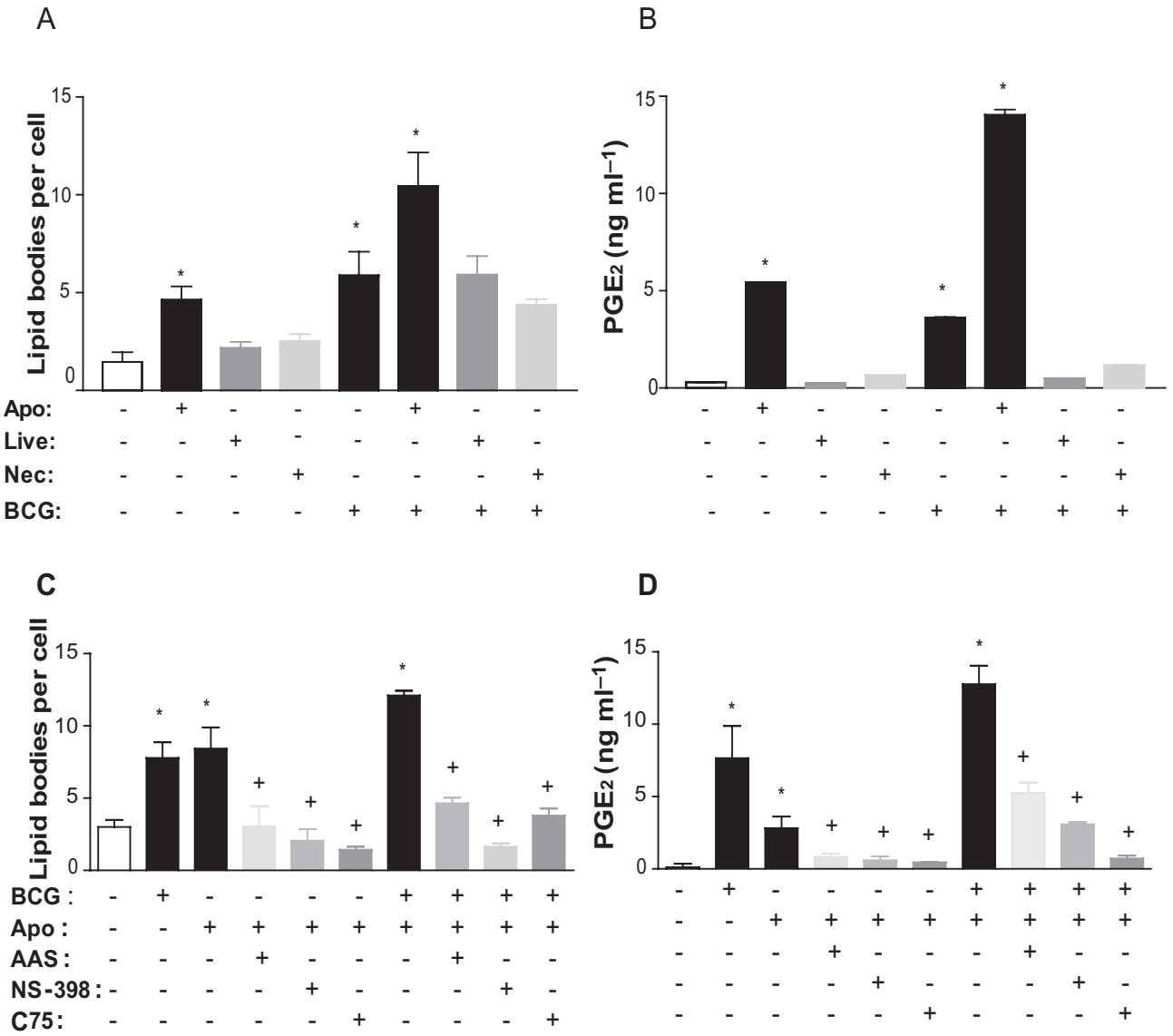

Fig. 6. NSAIDs, aspirin and NS-398 and fatty acid synthase inhibitor block lipid body formation and PGE_2 synthesis induced by BCG and apoptotic cells.
A and B. Peritoneal macrophages (1×10^6) were infected *in vitro* by BCG (moi, 5:1) for 2 h. Non-internalized BCG were removed, and the cells were stimulated by apoptotic, necrotic or live cells for 24 h at 37°C.
C and D. Macrophages stimulated by apoptotic cells and/or BCG were treated with 5 μM aspirin (ASA), 1 μM NS-398 or 5 μg ml^{-1} C75 for 24 h at 37°C. Vehicle (0.01% DMSO) was used as control.
Lipid bodies were enumerated after osmium staining (A and C), and PGE_2 were measured by EIA (B and D). Results are the mean ± SEM from three independent pools of three to five animals each. Statistically significant differences ($P < 0.05$) between control and stimulated groups are indicated by asterisks; differences between stimulated and treated groups are indicated by plus symbols (+).

Discussion

Neutrophils are cells rapidly recruited to sites of infection and injury, but their defence mechanisms that destroy and digest invading microorganisms are potentially deleterious to tissues (reviewed in Nathan, 2002). During inflammatory conditions, neutrophils spontaneously undergo apoptosis, and both neutrophil survival and apoptosis are profoundly influenced by the inflammatory milieu. Manipulation of these processes is likely to be a key therapeutic strategy in the management of inflammatory diseases (reviewed in Walker *et al*., 2005).

It has been recently demonstrated that human neutrophils undergo rapid apoptosis *in vitro* when stimulated with *M. tuberculosis* through mechanisms dependent on TLR2 and p38 MAPK pathway (Kasahara *et al*., 1998; Aleman *et al*., 2004). Here, we demonstrated that pleural BCG infection *in vivo* induces apoptosis in more than

© 2008 The Authors
Journal compilation © 2008 Blackwell Publishing Ltd,

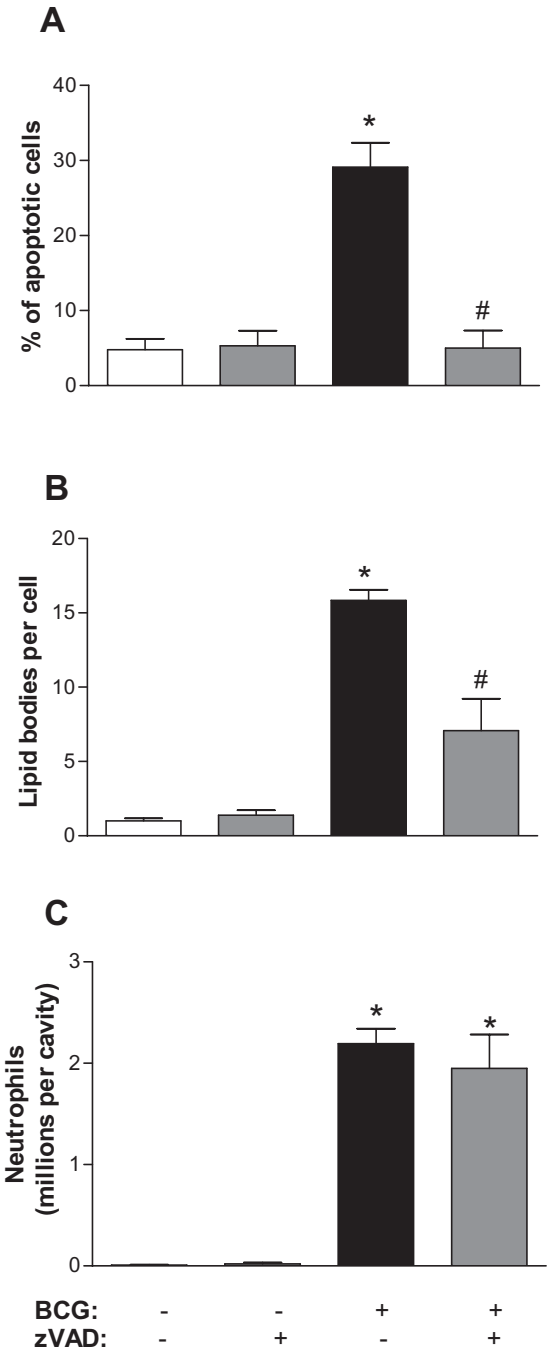

Fig. 7. Effect of apoptosis inhibition on macrophage lipid body formation and neutrophil migration in infected animals. (A) Percentages of apoptotic neutrophils, (B) macrophage lipid body formation and (C) neutrophils influx in control and infected groups after pre-treatment (5 min) with zVAD (caspase inhibitor) at 24 h of infection. Each bar represents the mean ± SEM from at least eight animals. Statistically significant ($P < 0.05$) differences between control and infected group are indicated by asterisks; differences between stimulated and treated group are indicated by a hash (#).

one-third of infiltrating neutrophils within 24 h. When analysed by TEM, these cells showed clear alterations associated with apoptosis. Moreover, by flow cytometry and electron microscopy we detected that the large majority of the apoptotic neutrophils were infected, suggesting that the apoptosis was induced after mycobacterial phagocytosis.

Our present ultrastructural analyses identified the presence of apoptotic neutrophils within macrophages. Apoptotic neutrophil recognition and clearance in the lung were shown to play critical functions in the resolution of the inflammatory response, by the removal of the inflammatory cells themselves, along with ingested organisms, and also by the generation of potent anti-inflammatory mediators (Henson, 2005). However, in infectious conditions the uptake of apoptotic cells by macrophages drives the replication of intracellular parasites and viruses through mechanisms dependent on TGF-β and PGE_2 (Freire-de-Lima *et al.*, 2000; 2006; Ribeiro-Gomes *et al.*, 2004; 2005; Xiao *et al.*, 2006). Accordingly, our work demonstrated that during BCG infection the uptake of apoptotic neutrophils by macrophages leads to enhanced anti-inflammatory mediator synthesis including TGF-β and PGE_2. The induction of TGF-β itself could be attributed to exposed phosphatidylserine on the apoptotic cells, which therefore may drive the balanced inflammatory mediator responses (Xiao *et al.*, 2006). Indeed, in response to apoptotic cells, macrophages rapidly release pre-formed TGF-β (McDonald *et al.*, 1999; Huynh *et al.*, 2002) followed by new synthesis and prolonged generatio of the active molecule. The combined production of the immunosuppressants PGE_2 and TGF-β1 may act to down-modulate host antimycobacterial immunity and thereby permit uncontrolled bacterial replication (Rangel Moreno *et al.*, 2002; Bonecini-Almeida *et al.*, 2004). In addition to the infection, apoptotic cells, through TGF-β synthesis, coordinately induce PGE_2 and suppress pro-inflammatory eicosanoid production and facilitate infection by intracellular pathogens (Fadok *et al.*, 1998; Freire-de-Lima *et al.*, 2000; 2006; Ribeiro-Gomes *et al.*, 2005).

Notably, macrophages from infected animals that ingested apoptotic cells exhibit highly increased numbers of cytoplasmic lipid bodies. Leukocyte lipid bodies are dynamic organelles which are formed by rapid and tightly regulated mechanisms triggered by different stimuli and pathological conditions including obesity-induced inflammation, ox-LDL- and LPS-induced inflammation or bacterial infection (Pacheco *et al.*, 2002; Silva *et al.*, 2002; de Assis *et al.*, 2003; Cinti *et al.*, 2005; D'Avila *et al.*, 2006; Pacheco *et al.*, 2007; Maya-Monteiro *et al.*, 2008). Under inflammatory conditions lipid bodies are sites of arachidonate compartmentalization and locales at which enzymatic events involved in arachidonate mobilization and oxidative metabolism take place (reviewed in Weller *et al.*, 1999;

© 2008 The Authors

Bozza *et al*., 2007). Recently, we have demonstrated increased lipid body numbers, cyclooxygenase-2 localization in lipid bodies and priming for prostaglandin production induced by BCG and also by the intracellular parasite, *T. cruzi*, in macrophages during *in vivo* experimental infection in rodents. Biogenesis of lipid bodies induced by these intracellular pathogens occurred through TLR-2 signalling and culminated with augment of PGE_2 synthesis (Melo *et al*., 2003; D'Avila *et al*., 2006). The present work suggests that lipid bodies in macrophages might participate in the enhanced formation of PGE_2 observed during apoptotic neutrophil uptake by macrophages in the acute BCG infection. Indeed, treatment with the pan-caspase inhibitor zVAD-fmk peptide was able to prevent the neutrophil apoptosis, and this fate reduced the lipid body formation induced during BCG infection *in vivo*.

Increased formation of eicosanoid has been observed during BCG infection and prostaglandins seem to play a role in the pathogenesis of BCG infections (Rangel Moreno *et al*., 2002; D'Avila *et al*., 2006). Different mechanisms may contribute to enhanced eicosanoid production during *in vivo* BCG infection. In fact, our results demonstrated that macrophages cultivated with apoptotic cells only (but not necrotic or living cells) presented augmented lipid body biogenesis and PGE_2 synthesis and priming for eicosanoid synthesis when stimulated *in vitro*. Accordingly, the inhibition of lipid body formation by treatment with aspirin, NS-398 or C75 led also to an inhibitory effect on PGE_2 production during BCG infection in the presence of apoptotic cells. We recently demonstrated that the inhibition of the PGE_2-derived lipid body formation by aspirin and NS-398 induced the enhancement of TNF-α production and a drastic reduction on IL-10 generation induced by BCG infection (D'Avila *et al*., 2006). Increased levels of PGE_2 favour intracellular pathogen growth, a phenomenon that could be reverted by treatment with COX-2 inhibitors (Freire-de-Lima *et al*., 2000; Rangel Moreno *et al*., 2002). In addition, the inhibition of lipid body formation by modulation of lipid metabolism through fatty acid inhibitor induced a similar effect to that obtained with NAIDS. Strikingly, although C75 is not an inhibitor of cyclooxygenase enzymatic activity it significantly inhibited PGE_2 production, thus suggesting that COX-2 compartmentalization within lipid bodies may play roles in the enhanced PGE_2 synthetic capacity induced by apoptotic neutrophil uptake.

In addition to the observations that increased lipid body biogenesis during infection may favour pathogen growth by the modulation of host immune response leading to an anti-inflammatory milieu, pathogens may potentially mobilize lipid body content as part of their pathogenic mechanism and source of nutrients. Accordingly, *Pseudomonas aeruginosa*-derived phospholipase activity was demonstrated to mobilize AA from lipid bodies in respiratory epithelial cells as part of their pathogenic mechanism (Plotkowski *et al*., 2008). Moreover, intimate contact and/or co-option of lipid bodies into phagosomes has been observed during infections by intracellular pathogens, including mycobacterial infection, suggesting that intracellular pathogens target lipid bodies to enhance their survival and replication in host cells (Melo *et al*., 2003; Chen *et al*., 2005; D'Avila *et al*., 2006; 2008; Kumar *et al*., 2006; Cocchiaro *et al*., 2008). Recently, Neyrolles *et al*. (2006) demonstrated that mycobacteria can accumulate lipids derived from lipid bodies and survive in a non-replicating state inside adipocytes.

Collectively, our results suggest that infected apoptotic neutrophils may act as *Trojan horse* during mycobacterial infection being rapidly uptaken by macrophages and inducing a favourable environment for the bacteria to establish the infection. Accordingly, a similar phenomenon of neutrophil facilitation of macrophage infection has been shown to occur during *Leishmania* infection (reviewed in Laskay *et al*., 2008). Interestingly, Aleman *et al*. (2007) suggested that phagocytosis of non-infected apoptotic polymorphonuclear cells (PMN) impaired mycobacteria-induced maturation of dendritic cells; however, the phagocytosis of infected apoptotic PMN allowed the cross-presentation of mycobacterial antigens, demonstrating that the inflammatory milieu is subject to a fine balance between infected and non-infected apoptotic cells and may facilitate mycobacterial infection and/or dissemination.

In conclusion, we demonstrated the *in vivo* BCG infection induced early recruitment, activation and apoptosis of neutrophils in the inflammatory site. The phagocytosis of apoptotic neutrophils by macrophages synergizes with BCG infection inducing lipid body formation and production of anti-inflammatory mediators, such as PGE_2 and TGF-β. Thus, our findings suggest that the phagocytosis of apoptotic cells may favour bacteria persistence by promoting an anti-inflammatory environment with macrophage deactivation.

Experimental procedures

Reagents and antibodies

zVAD (OMe)-FMK was obtained from Calbiochem-Novabiochem (La Jolla, CA). Osmium tetroxide (OsO_4) was from Merck (Darmstadt, Germany). TACS Annexin-V FITC apoptosis detection Kit was from R&D Systems (Minneapolis, MN). Nile red, RPMI-1640 cell-culture medium and PKH26 Red Fluorescent cell linker Kit were from Sigma (St Louis, MO). Guinea pig polyclonal anti-ADRP (Research Diagnostics, Concord, MA) and normal guinea pig serum as control were used for EM (2 $\mu g\ ml^{-1}$) immunodetection studies. Secondary antibody for immuno-EM was an affinity-purified donkey anti-guinea pig Fab fragment conjugated to 1.4 nm gold (1:100; Nanogold®, Nanoprobes, Stony Brook, NY).

© 2008 The Authors
Journal compilation © 2008 Blackwell Publishing Ltd,

Animals

C57BL/6 mice weighing 20–25 g from both sexes were obtained from the Fundação Oswaldo Cruz (Rio de Janeiro, Brazil) breeding unit. Animals were bred and maintained under standard conditions in the breeding unit of the Oswaldo Cruz Foundation, Brazil. Animals were caged with free access to food and water in a room at 22–24°C and a 12 h light/dark cycle in the Department of Physiology and Pharmacodynamic animal facility until used. All protocols were approved by the Fundação Oswaldo Cruz animal welfare committee.

M. bovis *BCG*

Mycobacterium bovis BCG (Moreau strain) was kindly donated by Fundação Ataulpho de Paiva, Rio de Janeiro, Brazil (Benévolo-de-Andrade *et al*., 2005). The freeze-dried vaccine was stored at 4°C. BCG was re-suspended in physiologic solution just before use.

Mycobacterium *staining*

For fluorescent microscopy, BCG (50×10^6 bacilli ml^{-1}) were incubated with 3 μl of the component A (Live/Dead BacLight bacterial viability kit from Molecular Probes) and incubated at room temperature in the dark for 15 min. BCG was pelleted by centrifugation, washed and re-suspended in physiologic solution. For FACS analysis, BCG (50×10^6 bacilli ml^{-1}) were incubated with a solution of 4 μM of PKH26 dye (PKH26 Red Fluorescent cell linker Kit from Sigma) and incubated at room temperature in the dark for 2 min. To stop the staining reaction was added an equal total volume of heat-inactivated FBS and incubated for 1 min BCG was pelleted by centrifugation, washed and re-suspended in physiologic solution. Animals were infected i.pl. by fluorescent labelled BCG (5×10^6 bacilli per cavity). For light microscopy, cytocentrifuged smears from *in vivo* unstained BCG-infected group were fixed in methanol and stained with Kinyoun's carbol fuchsin as described by Lavallee (1973). The cells were observed under light microscopy in a 100× objective lens.

Pleurisy induced by BCG

Mice were i.pl. injected with 5×10^6 bacilli per cavity in 100 μl of sterile saline. Control animals received an equal volume (100 μl) of sterile saline only. After different time intervals (1 h to 15 days) the animals were killed by CO_2 inhalation and their thoracic cavities were washed with 1 ml of the heparinized PBS (10 UI ml^{-1}). One group of animals was i.pl. pre-treated with the pan-caspase inhibitor – zVAD – at 20 μg $cavity^{-1}$, 5 min before BCG injection.

Induction of apoptotic neutrophils

Murine neutrophils were obtained from the bone marrow. The marrow cavities from murine femurs were flushed with 3 ml of heparinized (10 UI ml^{-1}) Ca^{2+}/Mg^{2+}-free HBSS. Bone marrow cells were washed and re-suspended in 5 ml of Ca^{2+}/Mg^{2+}-free HBSS and placed on the top of a discontinuous Percoll gradient with densities of 40–72%. Cells were centrifuged for 1 h at 3500 r.p.m. Neutrophils were recovered from the interface (purity, > 95%). The cells were washed twice in 10 ml of Ca^{2+}-Mg^{2+}-free HBSS. The cells were suspended in complete RPMI medium and UV-irradiated at 254 nm for 10 min followed by culture in RPMI containing 10% heat-inactivated FBS at 37°C, 5% CO_2 for 4 h as described by Fadok *et al*. (1998). The cells exhibited more that 90% of apoptosis after Annexin-V staining. Viable cells were also frozen–thawed to obtain necrotic cells (Griffith *et al*., 1996).

In vitro *macrophage infection*

Peritoneal cells from naïve C57/BL6 mice were harvested by lavage with sterile RPMI cell-culture medium. Macrophages (1×10^6 cells ml^{-1}) were adhered in cover slides within culture plates (24 wells) overnight with RPMI-1640 cell-culture medium containing 2% FBS. The non-adherent cells were removed after two vigorous PBS washes. Macrophages were infected by BCG [multiplicity of infection (moi), 5:1] and/or treated with apoptotic, necrotic or living neutrophils (3:1) for 24 h at 37°C in CO_2 atmosphere. In inhibitory studies macrophages stimulated by apoptotic cells and/or BCG were treated with NAIDS, 5 μM aspirin (ASA) and 1 μM NS-398 or 5 μg ml^{-1} fatty acid synthase inhibitor (C75) for 24 h at 37°C. Vehicle (0.01% DMSO) was used as control. Viability was assessed by trypan blue exclusion at the end of each experiment and was always greater than 90%. Lipid bodies were enumerated after osmium staining.

Quantification of apoptotic and infected neutrophils

The pleural fluids from control and PKH26-labelled BCG groups were recovered with 1 ml of heparinized PBS (10 UI ml^{-1}). For FACS analysis, total cells were stained with TACS Annexin-V FITC apoptosis detection Kit, according to the manufacturer's instructions (R&D Systems, Minneapolis, MN). The cells were then washed with PBS and the analysis was performed using the CellQuest program in a FACS Calibur flow cytometer (BD Biosciences, San Jose, CA). At least 10^4 neutrophils were acquired per sample. All data were collected and displayed as number of apoptotic cells per cavity and also as percentage of Annexin-V (green) and/or PKH26 (red) positive neutrophils gated based on forward and scatter analysis. For microscopic analysis, neutrophils were purified under Percoll gradient as described above. Neutrophil apoptosis was detected *in situ* using TACS Annexin-V FITC apoptosis detection. At least 100 cells per group were analysed by fluorescence microscopy. Cells were considered apoptotic when presented Annexin-V-positive staining and propidium iodide-negative staining. Apoptosis of inflammatory cells was further confirmed by morphology in May-Grünwald-Giemsa stained cytocentrifuged smears considering cells apoptotic when their nuclei appeared round and darkly stained and lost segmentation. Apoptotic percentages obtained by these methods agreed within 5%.

Lipid body staining and enumeration

Different techniques were used for lipid body staining and quantification as described (D'Avila *et al*., 2006). For quantitative studies, cells were stained by osmium tetroxide. For the osmium staining the slides were rinsed in 0.1 M cacodylate buffer, incubated with 1.5% OsO_4 (30 min), rinsed in H_2O, immersed in 1.0%

© 2008 The Authors
Journal compilation © 2008 Blackwell Publishing Ltd,

thiocarbohydrazide (5 min), rinsed in 0.1 M cacodylate buffer, re-incubated in 1.5% OsO_4 (3 min), rinsed in distilled water and then dried for further analysis. The morphology of fixed cells was observed, and lipid bodies were enumerated by light microscopy with a 100× objective lens in 50 consecutive leukocytes in each slide. The operator responsible for counting was blinded to the codes for each slide. For fluorescent-labelled lipid bodies, cells recovered from the pleural cavities after 24 h of the infection by BCG and controls were incubated with Nile Red (1:10000 from a stock solution of 0.1 mg ml^{-1} in acetone) for 10 min at room temperature. After incubation, cells were washed twice in $HBSS^{-/-}$, cytospun onto slides and fixed in 3.7% formaldehyde at room temperature for 10 min.

Total and differential cell analysis

Total cells were counted in a Neubauer chamber after diluting in Turk solution (2% acetic acid solution). Differential analysis was performed by light microscopy in cytocentrifuged smears stained with May-Grünwald-Giemsa.

Conventional TEM

Pleural cells from control and infected animals (5×10^6 BCG per cavity for 1 h and 24 h) were centrifuged (2000 r.p.m., 5 min) and the pellets obtained were re-suspended and fixed in a mixture of freshly prepared aldehydes (1% paraformaldehyde and 1% glutaraldehyde) in 0.1 M phosphate buffer, pH 7.3 overnight at 4°C (Karnovsky, 1965). The cells were washed in the same buffer and embedded in molten 2% agar (Merck). Agar pellets containing the cells were post-fixed in a mixture of 1% phosphate-buffered osmium tetroxide and 1.5% potassium ferrocyanide (final concentration) for 1 h and processed for resin embedding (PolyBed 812, Polysciences, Warrington, PA). The sections were mounted on uncoated 200-mesh copper grids (Ted Pella, Redding, CA) before staining with uranyl acetate and lead citrate and viewed with a transmission electron microscope (EM 10; Zeiss, Germany) at 60 KV. Electron micrographs were randomly taken at the magnifications of 12 000–40 000× to study the entire cell profile and lipid body features. A total of 81 electron micrographs were evaluated.

Immunogold electron microscopy for ADRP

Cells were fixed as described above, and the agar pellets immersed in 30% sucrose in PBS overnight at 4°C, embedded in OCT compound (Miles, Elkhart, IN), and stored in –180°C liquid nitrogen for subsequent use. Pre-embedding immunolabelling was performed before standard EM processing (dehydration, infiltration, resin embedding and resin sectioning). Immunonanogold was performed on cryostat 10 μm sections mounted on glass slides. All steps were performed at room temperature as before (Melo *et al.*, 2005), using guinea pig polyclonal anti-ADRP (2 μg ml^{-1}) as specific primary antibody. The secondary antibody donkey anti-guinea pig conjugated to 1.4 nm gold was diluted at 1:100. Two controls were performed: (i) primary antibody was replaced by an irrelevant antibody and (ii) primary antibody was omitted. Specimens were examined as described for conventional TEM.

PGE_2 measurement

PGE_2 levels were measured directly in the supernatant from cell-free pleural lavage or *in vitro* stimulation at 24 h from control and stimulated groups. PGE_2 was assayed in the cell-free supernatant by enzyme-linked immunoassay (EIA), according to the manufacturer's instructions (Cayman Chemical).

TGF-β1 measurement

Supernatants from pleural cavities after 24 h of the infection by BCG and controls were collected and stored at –20°C until the day of analysis. TGF-β1 was measured using ELISA technique with specific monoclonal antibodies, according to manufacturer's instructions (Duo Set Kit from R&D systems).

Image acquisition

The images were obtained using an Olympus BX-FLA fluorescence microscope equipped with a Plan Apo 100× 1.4 Ph3 objective (Olympus Optical, Japan) and CoolSNAP-Pro CF digital camera in conjunction with Image-Pro Plus version 4.5.1.3 software (MediaCybernetics, San Diego, CA). The images were edited using Adobe Photoshop 5.5 software (Adobe Systems, San Jose, CA) Adobe Illustrator 10.0.

Statistical analysis

The results were expressed as mean ± SEM and were analysed statistically by means of ANOVA followed by the Neuman-Keuls–Student test with the levels of significance set at $P < 0.05$.

Acknowledgements

This work was supported by Conselho Nacional de Desenvolvimento Científico e Tecnológico (CNPq, Brazil), Fundação de Amparo à Pesquisa do Estado do Rio de Janeiro (FAPERJ, Brazil), Fundação de Amparo à Pesquisa do Estado de Minas Gerais (FAPEMIG, Brazil), PRONEX and PAPES (FIOCRUZ, Brazil). We thank Dr Adriana Vieira-de-Abreu for the assistance with FACS analysis. The authors are indebted to Dr Valéria Borges for comments on the work and manuscript.

References

Accioly, M.T., Pacheco, P., Maya-Monteiro, C.M., Carrossini, N., Robbs, B.K., Oliveira, S.S., *et al.* (2008) Lipid bodies are reservoirs of cyclooxygenase-2 and sites of prostaglandin-E_2 synthesis in colon cancer cells. *Cancer Res* **68:** 1732–1740.

Aleman, M., Garcia, A., Saab, M.A., De La Barrera, S.S., Finiasz, M., Abbate, E., and Sasiain, M.C. (2002) *Mycobacterium tuberculosis*-induced activation accelerates apoptosis in peripheral blood neutrophils from patients with active tuberculosis. *Am J Respir Cell Mol Biol* **27:** 583–592.

Aleman, M., Schierloh, P., de la Barrera, S.S., Musella, R.M., Saab, M.A., Baldini, M., *et al.* (2004) *Mycobacterium tuberculosis* triggers apoptosis in peripheral neutrophils

© 2008 The Authors
Journal compilation © 2008 Blackwell Publishing Ltd,

involving toll-like receptor 2 and p38 mitogen protein kinase in tuberculosis patients. *Infect Immun* **72:** 5150–5158.

Aleman, M., de la Barrera, S.S., Schierloh, P.L., Alves, L., Yokobori, N., Baldini, M., *et al.* (2005) In tuberculous pleural effusions, activated neutrophils undergo apoptosis and acquire a dendritic cell-like phenotype. *J Infect Dis* **192:** 399–409.

Aleman, M., de la Barrera, S., Schierloh, P., Yokobori, N., Baldini, M., Musella, R., *et al.* (2007) Spontaneous or *Mycobacterium tuberculosis*-induced apoptotic neutrophils exert opposite effects on the dendritic cell-mediated immune response. *Eur J Immunol* **37:** 1524–1537.

Antony, V.B., Sahn, S.A., Antony, A.C., and Repine, J.E. (1985) Bacillus Calmette-Guerin-stimulated neutrophils release chemotaxins for monocytes in rabbit pleural spaces and *in vitro*. *J Clin Invest* **76:** 1514–1521.

Appelberg, R. (2007) Neutrophils and intracellular pathogens: beyond phagocytosis and killing. *Trends Microbiol* **15:** 87–92.

Appelberg, R., Castro, A.G., Gomes, S., Pedrosa, J., and Silva, M.T. (1995) Susceptibility of beige mice to *Mycobacterium avium*: role of neutrophils. *Infect Immun* **63:** 3381–3387.

Armstrong, J.A., and Hart, P.D. (1971) Response of cultured macrophages to *Mycobacterium tuberculosis*, with observations on fusion of lysosomes with phagosomes. *J Exp Med* **134:** 713–740.

de Assis, E.F., Silva, A.R., Caiado, L.F., Marathe, G.K., Zimmerman, G.A., Prescott, S.M., *et al.* (2003) Synergism between platelet-activating factor-like phospholipids and peroxisome proliferator-activated receptor gamma agonists generated during low density lipoprotein oxidation that induces lipid body formation in leukocytes. *J Immunol* **171:** 2090–2098.

Benévolo-de-Andrade, T.C., Monteiro-Maia, R., Cosgrove, C., and Castello-Branco, L.R.R. (2005) BCG Moreau Rio de Janeiro – an oral vaccine against tuberculosis. *Mem Inst Oswaldo Cruz* **100:** 459–465.

Bonecini-Almeida, M.G., Ho, J.L., Boechat, N., Huard, R.C., Chitale, S., Doo, H., *et al.* (2004) Down-modulation of lung immune responses by interleukin-10 and transforming growth factor beta (TGF-beta) and analysis of TGF-beta receptors I and II in active tuberculosis. *Infect Immun* **72:** 2628–2634.

Bozza, P.T., Payne, J.L., Morham, S.G., Langenbach, R., Smithies, O., and Weller, P.F. (1996) Leukocyte lipid body formation and eicosanoid generation: cyclooxygenase-independent inhibition by aspirin. *Proc Natl Acad Sci USA* **93:** 11091–11096.

Bozza, P.T., Yu, W., Penrose, J.F., Morgan, E.S., Dvorak, A.M., and Weller, P.F. (1997) Eosinophil lipid bodies: specific, inducible intracellular sites for enhanced eicosanoid formation. *J Exp Med* **186:** 909–920.

Bozza, P.T., and Pacheco, P., Yu, W., and Weller, P.F. (2002) NS-398: cyclooxygenase-2 independent inhibition of leukocyte priming for lipid body formation and enhanced leukotriene generation. *Prostaglandins Leukot Essent Fatty Acids* **67:** 237–244.

Bozza, P.T., Melo, R.C.N., and Bandeira-Melo, C. (2007) Leukocyte lipid bodies regulation and function: contribution to allergy and host defense. *Pharmacol Ther* **113:** 30–49.

Cardona, P.J., Llatjos, R., Gordillo, S., Diaz, J., Ojanguren, I., Ariza, A., and Ausina, V. (2000) Evolution of granulomas in lungs of mice infected aerogenically with *Mycobacterium tuberculosis*. *Scand J Immunol* **52:** 156–163.

Chen, J.S., Chen, Y.L., Greenberg, A.S., Chen, Y.J., and Wang, S.M. (2005) Magnolol stimulates lipolysis in lipid-laden RAW 264.7 macrophages. *J Cell Biochem* **94:** 1028–1037.

Cinti, S., Mitchell, G., Barbatelli, G., Murano, I., Ceresi, E., Faloia, E., *et al.* (2005) Adipocyte death defines macrophage localization and function in adipose tissue of obese mice and humans. *J Lipid Res* **46:** 2347–2355.

Cocchiaro, J.L., Kumar, Y., Fischer, E.R., Hackstadt, T., and Valdivia, R.H. (2008) Cytoplasmic lipid droplets are translocated into the lumen of the *Chlamydia trachomatis* parasitophorous vacuole. *Proc Natl Acad Sci USA* **105:** 9379–9384.

D'Avila, H., Melo, R.C.N., Parreira, G.G., Werneck-Barroso, E., Castro-Faria-Neto, H.C., and Bozza, P.T. (2006) *Mycobacterium bovis* bacillus Calmette-Guerin induces TLR2-mediated formation of lipid bodies: intracellular domains for eicosanoid synthesis *in vivo*. *J Immunol* **176:** 3087–3097.

D'Avila, H., Almeida, P.E., Roque, N.R., Castro-Faria-Neto, H.C., and Bozza, P.T. (2007) Toll-like receptor-2-mediated C-C chemokine receptor 3 and eotaxin-driven eosinophil influx induced by *Mycobacterium bovis* BCG pleurisy. *Infect Immun* **75:** 1507–1511.

D'Avila, H., Maya-Monteiro, C.M., and Bozza, P.T. (2008) Lipid bodies in innate immune response to bacterial and parasite infections. *Int Immunopharmacol* **8:** 1308–1315.

Dvorak, A.M., and Monahan-Earley, R. (1992) *Diagnostic Ultrastructural Pathology I*. Boca Raton, Florida: CRC Press.

Dvorak, A.M., Dvorak, H.F., Peters, S.P., Shulman, E.S., MacGlashan, D.W., Jr, Pyne, K., *et al.* (1983) Lipid bodies: cytoplasmic organelles important to arachidonate metabolism in macrophages and mast cells. *J Immunol* **131:** 2965–2976.

Dvorak, A.M., Morgan, E., Schleimer, R.P., Ryeom, S.W., Lichtenstein, L.M., and Weller, P.F. (1992) Ultrastructural immunogold localization of prostaglandin endoperoxide synthase (cyclooxygenase) to non-membrane-bound cytoplasmic lipid bodies in human lung mast cells, alveolar macrophages, type II pneumocytes, and neutrophils. *J Histochem Cytochem* **40:** 759–769.

Eruslanov, E.B., Lyadova, I.V., Kondratieva, T.K., Majorov, K.B., Scheglov, I.V., Orlova, M.O., and Apt, A.S. (2005) Neutrophil responses to *Mycobacterium tuberculosis* infection in genetically susceptible and resistant mice. *Infect Immun* **73:** 1744–1753.

Fadok, V.A., Bratton, D.L., Konowal, A., Freed, P.W., Westcott, J.Y., and Henson, P.M. (1998) Macrophages that have ingested apoptotic cells *in vitro* inhibit proinflammatory cytokine production through autocrine/paracrine mechanisms involving TGF-beta, PGE2, and PAF. *J Clin Invest* **101:** 890–898.

Freire-de-Lima, C.G., Nascimento, D.O., Soares, M.B., Bozza, P.T., Castro-Faria-Neto, H.C., de Mello, G.C., *et al.* (2000) Uptake of apoptotic cells drives the growth of a pathogenic trypanosome in macrophages. *Nature* **403:** 199–203.

© 2008 The Authors
Journal compilation © 2008 Blackwell Publishing Ltd,

Freire-de-Lima, C.G., Xiao, Y.Q., Gardai, S.J., Bratton, D.L., Schiemann, W.P., and Henson, P.M. (2006) Apoptotic cells, through transforming growth factor-beta, coordinately induce anti-inflammatory and suppress pro-inflammatory eicosanoid and NO synthesis in murine macrophages. *J Biol Chem* **281:** 38376–38384.

Fulton, S.A., Martin, T.D., Redline, R.W., and Henry Boom, W. (2000) Pulmonary immune responses during primary *Mycobacterium bovis*-Calmette-Guerin bacillus infection in C57Bl/6 mice. *Am J Respir Cell Mol Biol* **22:** 333–343.

Griffith, T.S., Yu, X., Herndon, J.M., Green, D.R., and Ferguson, T.A. (1996) CD95-induced apoptosis of lymphocytes in an immune privileged site induces immunological tolerance. *Immunity* **5:** 7–16.

Haslett, C. (1997) Granulocyte apoptosis and inflammatory disease. *Br Med Bull* **53:** 669–683.

Haslett, C. (1999) Granulocyte apoptosis and its role in the resolution and control of lung inflammation. *Am J Respir Crit Care Med* **160:** S5–S11.

Henson, P.M. (2005) Dampening inflammation. *Nat Immunol* **6:** 1179–1181.

Hines, M.E., 2nd, Kreeger, J.M., and Herron, A.J. (1995) Mycobacterial infections of animals: pathology and pathogenesis. *Lab Anim Sci* **45:** 334–351.

Hirsch, C.S., Ellner, J.J., Blinkhorn, R., and Toossi, Z. (1997) *In vitro* restoration of T cell responses in tuberculosis and augmentation of monocyte effector function against *Mycobacterium tuberculosis* by natural inhibitors of transforming growth factor beta. *Proc Natl Acad Sci USA* **94:** 3926–3931.

Hsueh, W., Kuhn, C., 3rd, and Needleman, P. (1979) Relationship of prostaglandin secretion by rabbit alveolar macrophages to phagocytosis and lysosomal enzyme release. *Biochem J* **184:** 345–354.

Huynh, M.L., Fadok, V.A., and Henson, P.M. (2002) Phosphatidylserine-dependent ingestion of apoptotic cells promotes TGF-beta1 secretion and the resolution of inflammation. *J Clin Invest* **109:** 41–50.

Jones, G.S., Amirault, H.J., and Andersen, B.R. (1990) Killing of *Mycobacterium tuberculosis* by neutrophils: a nonoxidative process. *J Infect Dis* **162:** 700–704.

Karnovsky, M.J. (1965) A formaldehyde-glutaraldehyde fixative of high osmolarity for use in electron microscopy. *J Cell Biol* **27:** 137A–138A.

Kasahara, K., Sato, I., Ogura, K., Takeuchi, H., Kobayashi, K., and Adachi, M. (1998) Expression of chemokines and induction of rapid cell death in human blood neutrophils by *Mycobacterium tuberculosis*. *J Infect Dis* **178:** 127–137.

Keller, C., Hoffmann, R., Lang, R., Brandau, S., Hermann, C., and Ehlers, S. (2006) Genetically determined susceptibility to tuberculosis in mice causally involves accelerated and enhanced recruitment of granulocytes. *Infect Immun* **74:** 4295–4309.

Klegerman, M.E., Devadoss, P.O., Garrido, J.L., Reyes, H.R., and Groves, M.J. (1996) Chemical and ultrastructural investigations of *Mycobacterium bovis* BCG: implications for the molecular structure of the mycobacterial cell envelope. *FEMS Immunol Med Microbiol* **15:** 213–222.

Kumar, Y., Cocchiaro, J., and Valdivia, R.H. (2006) The obligate intracellular pathogen *Chlamydia trachomatis* targets host lipid droplets. *Curr Biol* **16:** 1646–1651.

Laskay, T., van Zandbergen, G., and Solbach, W. (2008) Neutrophil granulocytes as host cells and transport vehicles for intracellular pathogens: apoptosis as infection-promoting factor. *Immunobiology* **213:** 183–191.

Lavallee, P.W. (1973) A new fluorescence and Kinyoun's acid-fast stain. *Am J Clin Pathol* **60:** 428–429.

McDonald, P.P., Fadok, V.A., Bratton, D., and Henson, P.M. (1999) Transcriptional and translational regulation of inflammatory mediator production by endogenous TGF-beta in macrophages that have ingested apoptotic cells. *J Immunol* **163:** 6164–6172.

MacMicking, J., Xie, Q.W., and Nathan, C. (1997) Nitric oxide and macrophage function. *Annu Rev Immunol* **15:** 323–350.

Martineau, A.R., Newton, S.M., Wilkinson, K.A., Kampmann, B., Hall, B.M., Nawroly, N., *et al.* (2007) Neutrophil-mediated innate immune resistance to mycobacteria. *J Clin Invest* **117:** 1988–1994.

Maya-Monteiro, C.M., Almeida, P.E., D'Avila, H., Martins, A.S., Rezende, A.P., Castro-Faria-Neto, H., and Bozza, P.T. (2008) Leptin induces macrophage lipid body formation by a phosphatidylinositol 3-kinase- and mammalian target of rapamycin-dependent mechanism. *J Biol Chem* **283:** 2203–2210.

Melo, R.C.N., and Machado, C.R. (1998) Depletion of radiosensitive leukocytes exacerbates the heart sympathetic denervation and parasitism in experimental Chagas' disease in rats. *J Neuroimmunol* **84:** 151–157.

Melo, R.C.N., D'Avila, H., Fabrino, D.L., Almeida, P.E., and Bozza, P.T. (2003) Macrophage lipid body induction by Chagas disease *in vivo*: putative intracellular domains for eicosanoid formation during infection. *Tissue Cell* **35:** 59–67.

Melo, R.C.N., Perez, S.A., Spencer, L.A., Dvorak, A.M., and Weller, P.F. (2005) Intragranular vesiculotubular compartments are involved in piecemeal degranulation by activated human eosinophils. *Traffic* **6:** 866–879.

Melo, R.C.N., Fabrino, D.L., Dias, F.F., and Parreira, G.G. (2006) Lipid bodies: structural markers of inflammatory macrophages in innate immunity. *Inflamm Res* **55:** 342–348.

Menezes-de-Lima-Junior, O., Werneck-Barroso, E., Cordeiro, R.S., and Henriques, M.G. (1997) Effects of inhibitors of inflammatory mediators and cytokines on eosinophil and neutrophil accumulation induced by *Mycobacterium bovis* bacillus Calmette-Guerin in mouse pleurisy. *J Leukoc Biol* **62:** 778–785.

Nathan, C. (2002) Points of control in inflammation. *Nature* **420:** 846–852.

Neyrolles, O., Hernandez-Pando, R., Pietri-Rouxel, F., Fornes, P., Tailleux, L., Barrios Payan, J.A., *et al.* (2006) Is adipose tissue a place for Mycobacterium tuberculosis persistence? *PLoS ONE* **1:** e43.

Pacheco, P., Bozza, F.A., Gomes, R.N., Bozza, M., Weller, P.F., Castro-Faria-Neto, H.C., and Bozza, P.T. (2002) Lipopolysaccharide-induced leukocyte lipid body formation *in vivo*: innate immunity elicited intracellular loci involved in eicosanoid metabolism. *J Immunol* **169:** 6498–6506.

Pacheco, P., Vieira-de-Abreu, A., Gomes, R.N., Barbosa-Lima, G., Wermelinger, L.B., Maya-Monteiro, C.M., *et al.* (2007) Monocyte chemoattractant protein-1/CC chemokine

© 2008 The Authors
Journal compilation © 2008 Blackwell Publishing Ltd,

ligand 2 controls microtubule-driven biogenesis and leukotriene B_4-synthesizing function of macrophage lipid bodies elicited by innate immune response. *J Immunol* **179:** 8500–8508.

Pedrosa, J., Saunders, B.M., Appelberg, R., Orme, I.M., Silva, M.T., and Cooper, A.M. (2000) Neutrophils play a protective nonphagocytic role in systemic *Mycobacterium tuberculosis* infection of mice. *Infect Immun* **68:** 577–583.

Penido, C., Vieira-de-Abreu, A., Bozza, M.T., Castro-Faria-Neto, H.C., and Bozza, P.T. (2003) Role of monocyte chemotactic protein-1/CC chemokine ligand 2 on gamma delta T lymphocyte trafficking during inflammation induced by lipopolysaccharide or *Mycobacterium bovis* bacille Calmette-Guerin. *J Immunol* **171:** 6788–6794.

Plotkowski, M.C., Brandão, B.A., Assis, M.C., Feliciano, L.F.P., Saliba, A.S., Raymond, B., *et al.* (2008) Lipid body mobilization in the ExoU-induced release of inflammatory mediators by airway epithelial cells. *Microb Pathog* **45:** 30–37.

Rangel Moreno, J., Estrada Garcia, I., De La Luz Garcia Hernandez, M., Aguilar Leon, D., Marquez, R., and Hernandez Pando, R. (2002) The role of prostaglandin E_2 in the immunopathogenesis of experimental pulmonary tuberculosis. *Immunology* **106:** 257–266.

Ribeiro-Gomes, F.L., Otero, A.C., Gomes, N.A., Moniz-De-Souza, M.C., Cysne-Finkelstein, L., Arnholdt, A.C., *et al.* (2004) Macrophage interactions with neutrophils regulate *Leishmania major* infection. *J Immunol* **172:** 4454–4462.

Ribeiro-Gomes, F.L., Moniz-de-Souza, M.C., Borges, V.M., Nunes, M.P., Mantuano-Barradas, M., D'Avila, H., *et al.* (2005) Turnover of neutrophils mediated by Fas ligand drives *Leishmania major* infection. *J Infect Dis* **192:** 1127–1134.

Silva, A.R., de Assis, E.F., Caiado, L.F., Marathe, G.K., Bozza, M.T., McIntyre, T.M., *et al.* (2002) Monocyte chemoattractant protein-1 and 5-lipoxygenase products recruit leukocytes in response to platelet-activating factor-like lipids in oxidized low-density lipoprotein. *J Immunol* **168:** 4112–4120.

Walker, A., Ward, C., Taylor, E.L., Dransfield, I., Hart, S.P., Haslett, C., and Rossi, A.G. (2005) Regulation of neutrophil apoptosis and removal of apoptotic cells. *Curr Drug Targets Inflamm Allergy* **4:** 447–454.

Weller, P.F., and Dvorak, A.M. (1985) Arachidonic acid incorporation by cytoplasmic lipid bodies of human eosinophils. *Blood* **65:** 1269–1274.

Weller, P.F., Ackerman, S.J., Nicholson-Weller, A., and Dvorak, A.M. (1989) Cytoplasmic lipid bodies of human neutrophilic leukocytes. *Am J Pathol* **135:** 947–959.

Weller, P.F., and Bozza, P.T., Yu, W., and Dvorak, A.M. (1999) Cytoplasmic lipid bodies in eosinophils: central roles in eicosanoid generation. *Int Arch Allergy Immunol* **118:** 450–452.

Werneck-Barroso, E., Moura, A.C., Monteiro, M.M., Menezes de Lima Junior, O., de Meirelles, M.N., and Henriques, M.G. (2000) Distinct ability to accumulate eosinophils during the inflammatory cellular response to *M. bovis* BCG in the mouse pleural cavity. *Inflamm Res* **49:** 206–213.

Xiao, Y.Q., Freire-de-Lima, C.G., Janssen, W.J., Morimoto, K., Lyu, D., Bratton, D.L., and Henson, P.M. (2006) Oxidants selectively reverse TGF-beta suppression of proinflammatory mediator production. *J Immunol* **176:** 1209–1217.

Yu, W., Bozza, P.T., Tzizik, D.M., Gray, J.P., Cassara, J., Dvorak, A.M., and Weller, P.F. (1998) Co-compartmentalization of MAP kinases and cytosolic phospholipase A_2 at cytoplasmic arachidonate-rich lipid bodies. *Am J Pathol* **152:** 759–769.

© 2008 The Authors
Journal compilation © 2008 Blackwell Publishing Ltd,